Agromet 36 (1): 51-59, 2022

Agromet
journal.ipb.ac.id/index.php/agromet
ISSN : 0126 - 3633

Land Use Change Impact on Normalized Difference Vegetation Index, Surface Albedo, and Heat Fluxes in Jambi Province: Implications to Rainfall

Siti Nadia Nurul Azizah, Tania June, Resti Salmayenti, Ummu Ma'rufah, Yonny Koesmaryono
Department of Geophysics and Meteorology, IPB University, Bogor 16680, West Java, Indonesia

ARTICLE INFO

Received
27 January 2022

Revised
9 June 2022

Accepted for Publication
10 June 2022

Published
27 June 2022

doi: 10.29244/j.agromet.36.1.51-59

Correspondence:
Tania June
Department of Geophysics and Meteorology, IPB University, Bogor 16680, West Java, Indonesia
Email: taniajune@apps.ipb.ac.id

ABSTRACT

Jambi covers various land uses with different characteristics related to biogeophysical cycle. Land use plays an important role in the atmosphere-surface interaction and energy balance partition, which influenced rainfall pattern. Two proxies widely used to differentiate various land uses are albedo and normalized difference vegetation index (NDVI). However, study on albedo and NDVI relationship with rainfall in Jambi is still limited. This study aims to analyze the correlation of NDVI and albedo with rainfall and their distribution in Jambi and Muaro Jambi in 2013 and 2017. The research used Landsat 8 OLI TIRS satellite image data to derived NDVI and albedo, and CHIRPS data for rainfall. A simple linear regression was used to calculate the correlation of NDVI and albedo with rainfall. The results showed that the distribution of albedo for each land use class from the lowest to the highest was forest, plantation, cropland, shrubs, and settlements, respectively. On the contrary, the distribution of NDVI and rainfall is the inverse to albedo. Albedo and NDVI had a strong influence on rainfall through surface energy balance partition. This was indicated by the high R-square between albedo and rainfall (0.99) and between NDVI and rainfall (0.97). Increasing upward latent heat flux from the land surface to atmosphere leads to a rainfall increase. In other words, rainfall may also increase with the decrease in albedo, increase in NDVI, or land use change.

KEYWORDS
biogeophysics, energy partitioning, landsat-8, rainfall distribution, spatial analysis

INTRODUCTION

Land use plays an important role on the surface biogeophysical cycle. Each land use class has specific surface biophysical characteristics such as albedo, leaf area index (LAI), and surface roughness (Burakowski et al., 2018). These biophysical characteristics affect as the surface energy balance, water balance, and carbon cycle (Winckler et al., 2019). Surface energy partition and water balance control the condition of the atmosphere such as boundary layer depth, dynamic air flow, and cloud formation, which also led to rainfall (Fast et al., 2019).

Jambi Province covers an area of 53,435 km^2 with a large proportion of vegetation and forest (June et al., 2018b). It has a high annual rainfall (2500-4000 mm/year) with a monsoonal rainfall pattern. The wet season is in October-April, and the dry season is in June-August. However, there was a decreasing trend in the total area of forest (Rustiadi et al., 2018). Jambi Environmental Agency (BLHD 2018), reported that 366,964 ha of forest have been converted to other uses. Another research in the eastern lowland of Sumatra including Jambi, which has extensive coastal peatlands, revealed that there was a very high annual deforestation rate (Miettinen et al., 2011). This decreasing trend will influence the distribution of land use, which in turn may also alter the biogeophysical process in the land surface.

Previous findings in a high latitude forest revealed that increased deforestation rate or decreased NDVI will lead to increased albedo (Fusami et al., 2020; Scott et al., 2018). Research in tropical forest also reported that deforestation resulted in

decreased NDVI (Othman et al., 2018). In addition, Leite-Filho et al., (2021) stated that decreased evapotranspiration and rainfall pattern change in the Amazon Forest was caused by deforestation. From those studies, it is assumed that normalized difference vegetation index (NDVI) score can represent various land use class. NDVI was calculated from a mathematical equation using the red band and the NIR band in satellite data such as Landsat 8 OLI TIRS to indicate the presence of vegetation cover. This index is mainly influenced by land area covered by vegetation and the canopy density. NDVI may represent Leaf Area Index (LAI), a parameter to calculate plant maximum evapotranspiration and local rainfall (Oliveira et al., 2018). Therefore, this study aims to analyze the correlation between albedo and NDVI with rainfall and their distribution in various land use. This study also analyzed the effect of land use change and its implication to rainfall pattern in Jambi.

RESEARCH METHODS

Research Site

The research site was carried out in Muaro Jambi Regency and Jambi City. Land use class in the research site was based on Ministry of Forestry and Environment, Republic of Indonesia (2017). This classification was further grouped as forest, plantation, cropland, shrubs, and settlements. Secondary dryland forest, primary mangrove forest, secondary mangrove forest, primary swamp forest, secondary swamp forest, and plantation forest were grouped as forest. Plantation, cropland, and dryland farming were grouped as cropland. Swamp, savanna, rice field, shrub swamp, and shrubs were grouped as shrubs. Lastly, open field, built-up land, mines, and settlements were grouped as settlement.

Data Source

The data used in this study consisted of satellite data from Landsat-8 OLI TIRS, rainfall data from Climate Hazards Group InfraRed Rainfall with Station (CHIRPS) and OGIMET, and land cover map from Ministry of Forestry and Environment Indonesia (2013 & 2017). The satellite data from Landsat-8 OLI-TIRS (path/row 125/61 in 2013 and January 2017) had a spatial resolution of 30 m and temporal resolution of 16 days. This data was used to calculate surface albedo and LAI. The rainfall data used from CHRIPS was monthly rainfall in January 2013 and 2017 with a spatial resolution of 5 km. January is considered as wet month with rainfall amount >200 mm. Monthly rainfall station data in January 2013 and 2017 obtained from OGIMET was used to validate CHIRPS data. The meteorological station selected was Sultan Thaha Meteorological Station. Land cover map from Ministry of Forestry and Environment in 2013 and 2017 was used to describe land use distribution in the research site.

Preprocessing of Satellite Image Data

Landsat-8 satellite data was retrieved and geometrically corrected using Google Earth Engine (GEE). Afterwards, top of atmosphere (ToA) reflectance was corrected using radiometric correction (Yanuar et al., 2018), as shown in Equation 1.

$$\lambda' = M\rho Q_{cal} + A\rho \quad (1)$$

Where ρλ' is ToA reflectance, Mρ is reflectance_mult_band_x, Aρ is reflectance_add_band_x, and Qcal is the digital number stored in the metadata.

The value of digital number due to the sun position was corrected using ToA reflectance with the angle of the sun (Yanuar et al., 2018), as shown in Equation 2.

$$\rho\lambda = \frac{\rho\lambda'}{\cos(\theta_{SZ})} = \frac{\rho\lambda'}{\sin(\theta_{SE})} \quad (2)$$

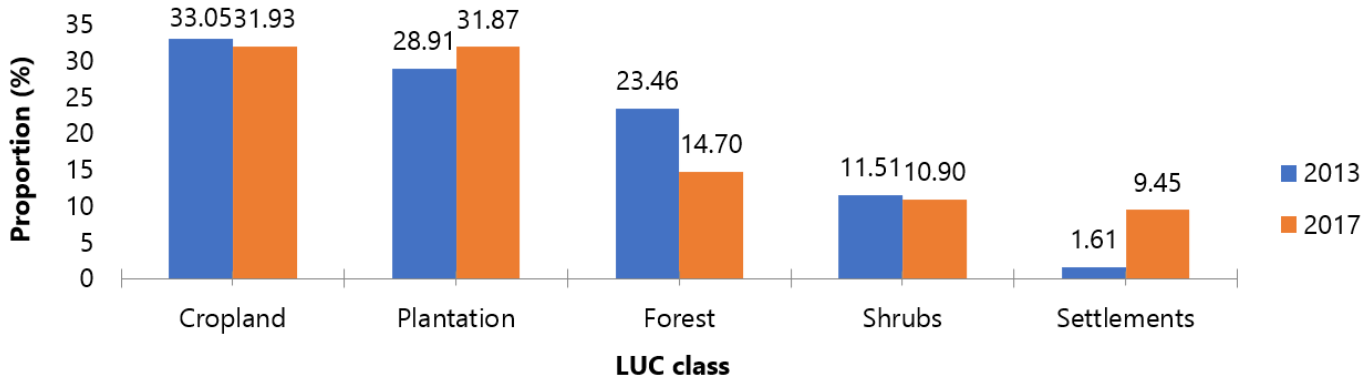

Figure 1. Proportion of land cover class in the study site in 2013 and 2017

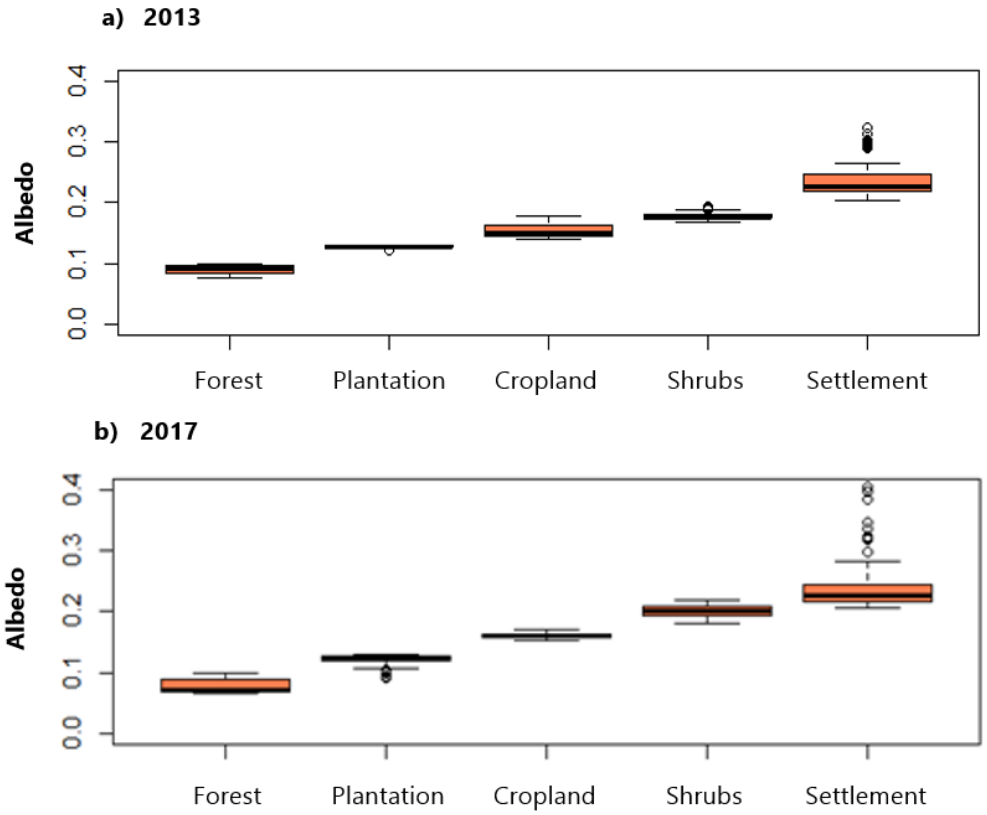

Figure 2. Distribution of albedo for each land cover class in the study site in a) 2013 and b) 2017

Where ρλ is ToA reflectance, θ_{SE} is the sun's elevation angle, and θ_{SZ} is the sun's zenith angle.

Spatial Processing of Albedo

To calculate surface albedo from Landsat-8 satellite imagery data, ToA reflectance of band 1, band 3, band 4, band 5, and band 7 is used. Equation 3 is the modified formula to calculate albedo using Landsat 8 from its previous version of Landsat 7 (Liang et al., 2003).

$$\alpha = \frac{0.356\rho_1+0.130\rho_3+0.373\rho_4+0.085\rho_5+0.072\rho_7-0.0018}{0.356+0.130+0.373+0.085+0.072} \quad (3)$$

Where ρ is the ToA reflectance of the specified band.

Normalized Difference Vegetation Index

NDVI is a widely used method to show differences in vegetation density in the land surface (Artikanur and June, 2019). Spectral bands used to calculate NDVI in Landsat 8 are band 5 (near infrared) and 4 (red) as formulated in Equation 4 (Jensen and Lulla, 1987).

$$NDVI = \frac{NIR-Red}{NIR+Red} \quad (4)$$

Heat Fluxes

Sensible heat (H) and latent heat (LE) fluxes are calculated using the energy balance (Rn) concept and Bowen ratio (β) method as formulated in Equation 5 and 6.

$$H = \frac{\beta\,(Rn-G)}{(\beta+1)} \quad (5)$$

$$LE = \frac{(Rn-G)}{(\beta+1)} \quad (6)$$

Where Rn is net radiation, G is soil heat flux, and β is Bowen ratio.

Rainfall Analysis

This study used monthly rainfall of January in 2013 and 2017. The first step to be carried out was rainfall bias correction. The correction was performed using the average ratio method (Lenderink et al., 2007), as shown in Equation 5.

$$P*model = Pmodel \times \frac{\mu m\ P\ obs}{\mu m\ Pmodel} \quad (7)$$

Where P_{model} is rainfall data from CHIRPS, μm P_{obs} is the mean monthly rainfall of observations, and μm P_{model} is the average monthly rainfall of CHIRPS.

Correlation Analysis

Relationship between NDVI, albedo, and rainfall was analyzed using a simple linear regression. The equation of simple linear regression model was shown in Equation 6.

$$Y = \alpha+\beta X + \varepsilon \quad (8)$$

Where Y is the dependent variable that is rainfall, X is the independent variable that is albedo and NDVI, ε is the error, and α is the regression parameter. Then T test and assumption test (normal test, homogeneity test of variance, and independent residual test) were carried out on the regression model.

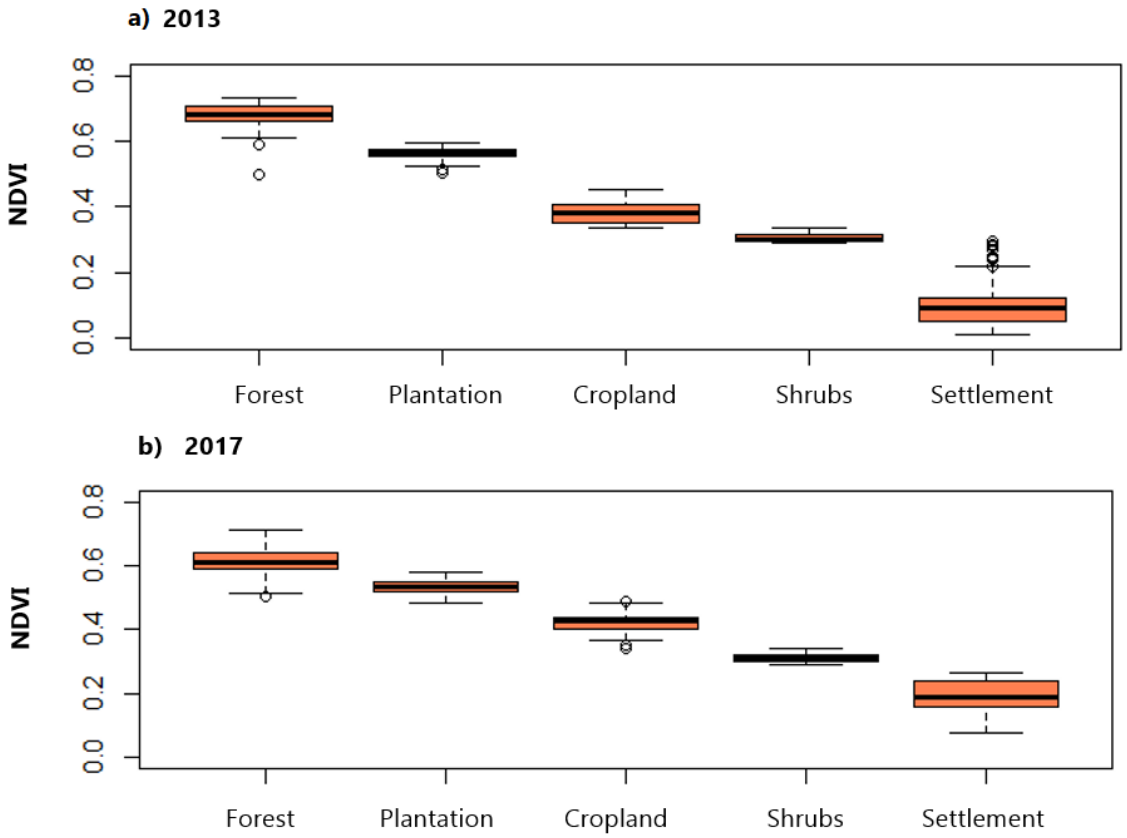

Figure 3. Distribution of NDVI for each land cover class in the study site in a) 2013 and b) 2017

RESULTS AND DISCUSSION

Land Use Types in the Study Area

Muaro Jambi and Jambi City covers an extensive land use area of agriculture, plantation, forest, shrub, and settlement. Cropland had the largest proportion in Muaro Jambi, which ranges from 33.05% of the total area in 2013 to 31.93% in 2017 (Figure 1). Mostly, agricultural crops cultivated in Muaro Jambi consists of horticultural crops and seasonal or annual fruit crops (BPS 2018). After cropland, plantation for rubber, oil palm, coffee, cocoa, and areca nut had the second-largest proportion in the region (BPS, 2018). Figure 1 also showed that there was a slight difference between proportion of each land use in 2013 and 2017, indicating land use change. Forest area decrea-

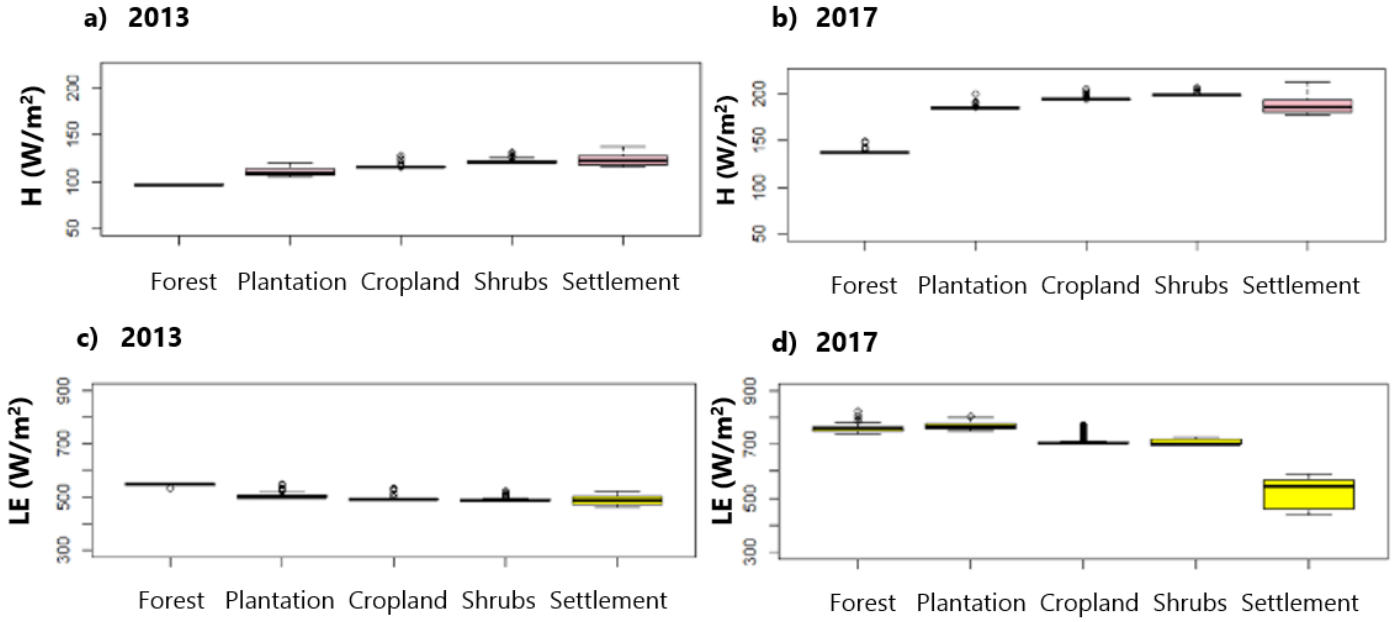

Figure 4. Distribution of sensible heat (H) in a) 2013 and b) 2017, and latent heat (LE) in c) 2013 and d) 2017 for each land cover class in the study site

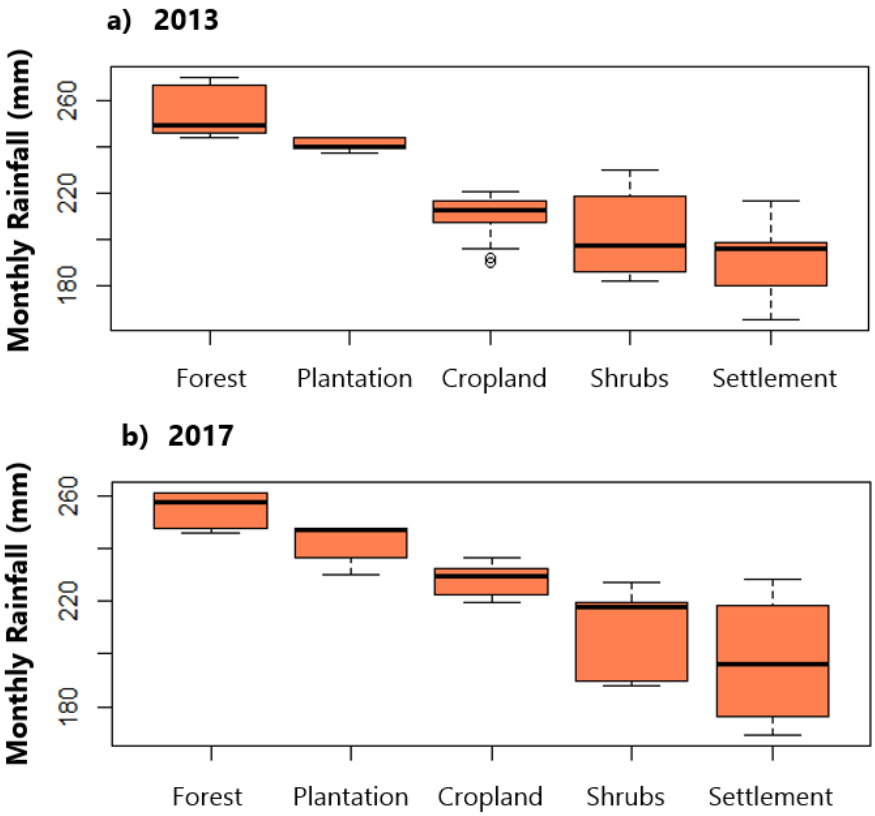

Figure 5. Distribution of monthly rainfall for each land cover class in the study site in a) 2013 and b) 2017

sed by 8.76%, followed by cropland (1.12%) and shrubs (0.6%). On the other hand, plantation and settlement area increased by 2.96% and 7.84%, respectively. According to Sabajo et al., (2017), the forest area was mostly converted due to the expansion of plantation. This was also supported by Rustiadi et al., (2018), who stated that plantation, especially oil palm plantation, may support the economy and provide employment for local communities, hence why the expansion occurred rapidly.

Distribution of Surface Albedo

Both in 2013 and 2017, settlement had the largest value range of albedo, along with an increase in its standard deviation. The large albedo value range was due to various distinct surface characteristics covered by the settlement class. Albedo mainly influenced by colour, texture, and wetness of an object. Thus, surface heterogeneity will result in a more varied albedo value. According to BPS (2018), settlement in Jambi consisted of road, building, farm area, industrial site, and transportation infrastructure. Land with vegetation cover, including forest, plantation, cropland, and shrub had an overall lower albedo compared to settlement and relatively smaller albedo value range (Figure 2). These land cover classes cover a more homogenous surface with similar characteristics. forest had the lowest albedo compared to the other land cover classes because of dense vegetation covering the surface. Cropland and shrub classes have a higher albedo than forest and plantation because the vegetation cover was less dense. Low albedo value implied that the surface absorbs more solar radiation than it reflects.

Distribution of NDVI

The distribution pattern of NDVI was inversely proportional to albedo (Figure 3). According to Artikanur and June (2019), a direct inversed relationship between albedo and LAI affects the NDVI value. Forest had the highest NDVI value, followed by plantation, agriculture, shrubs, and settlement, respectively. This was in line with Zaitunah et al., (2018), who reported that settlement especially in urban area had low NDVI values. Similar to previous results in albedo distribution, the settlement had the highest standard deviation of NDVI in 2013 and 2017. A high NDVI standard deviation indicated the diversity of red and infrared wavelength reflectance from the surface. This due to the same cause as in albedo, which is surface heterogeneity. In addition, there were also built-up lands in Muaro Jambi, which was surrounded by plantations or cropland (BPS, 2018), resulting in the diversity of the surface reflectance.

Distribution of Sensible Heat (H) and Latent Heat (LE) Fluxes

Sensible heat (H) distribution was inversely proportional to latent heat (LE) (Figure 4). A highly ve-

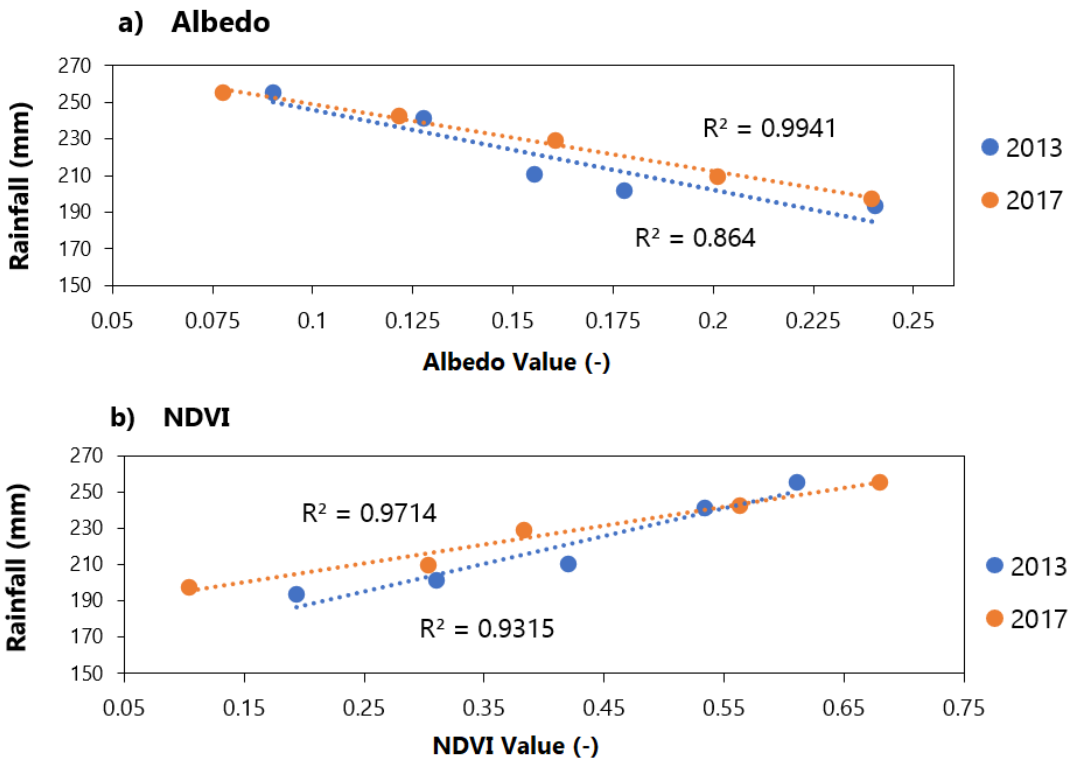

Figure 6. Correlation of rainfall and a) albedo and b) NDVI in the study site in 2013 and 2017

getated area (indicated by high NDVI value in Figure 3) will have a lower H value and higher LE value compared to less vegetated area. Accordingly, settlement had the highest H and lowest LE, followed by shrubs, cropland, plantation, and forest (Figure 4). The increasing rate of latent heat flux was recorded higher than increasing rate of sensible heat flux, in line with (Zeng and Zhang, 2020). However, the average value of H and LE were both increased in 2017 compared to 2013 (Figure 4). Similar to previous results, land use also plays a major role in altering this partitioning of latent heat and sensible heat fluxes (de Oliveira et al., 2019). The vegetation cover affects how the surface manage water vapor. Increasing upward latent heat flux from the land surface to atmosphere leads to a rainfall increase. In a highly vegetated area where upward latent heat flux is also high, there will be higher chance of low clouds formation, associated with increased evapotranspiration (de Oliveira et al., 2019).

Distribution of Rainfall

The rainfall distribution pattern was the same as NDVI. High NDVI score may indicate a dense canopy, causing high evapotranspiration from the surface that contributes to increased water vapour in the atmosphere. In this study, highest rainfall occurred in forest. This was also supported by previous analysis conducted in tropical region by Deb et al., (2018), who reported that in both wet and dry seasons, highest total rainfall was in forest. Besides having high NDVI leading to high evapotranspiration, forest also had lowest albedo. Low albedo indicated high absorption of solar radiation resulting in high available energy.

Since forest had higher soil moisture than other land cover classes, most available energy will be partitioned into latent heat flux rather than sensible heat flux. Latent heat flux can increase water vapour in the atmosphere, which later accelerate the convective cloud formation (Takahashi et al., 2017). In addition, forest also has high surface roughness that can increase turbulence. Turbulence can transfer energy from the surface to the atmosphere, leaving the surface to be colder. The available energy will mostly be used for evaporation rather than warming up the surface, resulting in lower surface temperature (Fast et al., 2019). On the contrary, low vegetated area such as settlement led to high surface temperature because most of the energy will be used to warm up the surface rather than for evaporation. Low evaporation will delay cloud formation because of limited water mass and cold pools (Fast et al., 2019).

High surface temperature in the settlement created a low-pressure area thus water vapour from the surrounding vegetated area will be transported into the settlement. This caused spatial variation of rainfall in the settlement, in accordance with Sabajo et al., (2017) who revealed that high variation in surface temperature lowlands was due to higher NDVI and lower albedo. There was a flow of moist air from the surrounding vegetated area in the lowland, which has a lower temperature and higher air pressure. This resulted in variations in rainfall on high built-up land.

Correlation of Albedo and NDVI with Rainfall

The correlation of albedo and NDVI with rainfall in 2013 and 2017 is presented in Figure 5. Albedo and rainfall had an inversed relationship, meaning that low albedo caused high rainfall and vice versa. In contrast, NDVI and rainfall had a linear relationship, meaning that high NDVI caused high rainfall and vice versa. The coefficient of determination (R^2) between albedo and rainfall was lower in 2013 (0.86) than in 2017 (0.99). Similarly, the R^2 of NDVI and rainfall was also lower in 2013 (0.93) than in 2017 (0.97). A T-test with p-value of 0.02 implied that there is a relationship between albedo and rainfall. For the normal test, p-value is 0.15 implied that the remainder is normally distributed. The homogeneity test of variance is 0.54, indicated homogeneous residual variance. The independent residual test is 0.12, implied independent residual. Therefore, it was presumed that the regression model had met all assumptions, and that there was a relationship between albedo and rainfall. The simple linear regression model related to the relationship between NDVI and rainfall also showed the same result. The regression model had met all assumptions, and there was a relationship between NDVI and rainfall.

There is a direct dependence of available energy on various surface parameters such as albedo and NDVI (Oliveira et al., 2018). Albedo is one of the radiation balance components, and NDVI strongly correlates to evapotranspiration and surface temperature (Artikanur and June, 2019). Rainfall itself has an important effect on the energy balance (Abera et al., 2020), in which it can affect the dynamics of sensible heat flux (H) and latent heat flux (LE) via the availability of surface water (June et al., 2018). In addition, rainfall also influences soil temperature (Li et al., 2019). This is in accordance with the condition that decreasing albedo and increasing NDVI will impact increasing rainfall.

CONCLUSIONS

The albedo in Muaro Jambi and Jambi City in January was lowest in forest, followed by plantation, cropland, shrubs, and settlement. In contrast, the NDVI was highest in forest, followed by plantation, cropland, shrubs, and settlement. Land use change from 2013 to 2017 led to increasing variance of albedo, NDVI, sensible and latent heat flux, and rainfall. The coefficient of determination between albedo and rainfall in 2013 was 0.86, while for NDVI and rainfall 0.93. Not much different, the coefficient of determination between albedo and rainfall in 2017 was 0.99, while for NDVI and rainfall 0.97. There was a linear relationship between NDVI and rainfall, and an inversed relationship between albedo and rainfall. Among all land cover classes, the settlement had a highest variation of rainfall due to high variation of surface characteristics (albedo, NDVI, sensible and latent heat flux). The settlement also had high albedo that leads to increased surface temperature, sensible and latent heat flux. Increasing upward latent heat flux from the land surface to atmosphere leads to a rainfall increase. Rainfall increased with the decrease in albedo and increase in latent heat flux and NDVI. The various land use change also affects rainfall pattern change.

ACKNOWLEDGEMENT

The authors would like to thank the CRC990 Efforts Projects for the support during fieldwork, and the provider of data resources including the Ministry of Environment and Forestry for the land use map, Google Earth Engine for the access to Landsat data, also IRIDL and OGIMET for the precipitation data.

REFERENCES

Abera, T.A., Heiskanen, J., Pellikka, P.K.E., Maeda, E.E., 2020. Impact of rainfall extremes on energy exchange and surface temperature anomalies across biomes in the Horn of Africa. Agric. For. Meteorol. 280, 107779. https://doi.org/10.1016/j.agrformet.2019.107779

Artikanur, S.D., June, T., 2019. Surface Temperature and Heat Fluxes: Comparison between Natural Forest and Oil Palm Plantation in Jambi Province Using Surface Energy Balance Algorithm for Land (SEBAL). Agromet 33, 62–70. https://doi.org/10.29244/j.agromet.33.2.62-70

BLHD, 2018. Buku Data Status Lingkungan Hidup Daerah Provinsi Jambi. Badan Lingkungan Hidup Daerah Provinsi Jambi.

BPS, 2018a. Kabupaten Muaro Jambi dalam Angka 2018. Badan Pusat Statistik.

BPS, 2018b. Kota Jambi dalam Angka 2018. Badan Pusat Statistik.

Burakowski, E., Tawfik, A., Ouimette, A., Lepine, L., Novick, K., Ollinger, S., Zarzycki, C., Bonan, G., 2018. The role of surface roughness, albedo, and Bowen ratio on ecosystem energy balance in the Eastern United States. Agric. For. Meteorol. 249, 367–376. https://doi.org/10.1016/j.agrformet.2017.11.030

de Oliveira, G., Brunsell, N.A., Moraes, E.C., Shimabukuro, Y.E., dos Santos, T. V., von Randow, C., de Aguiar, R.G., Aragao, L.E.O.C., 2019. Effects of land-cover changes on the partitioning of surface energy and water fluxes in Amazonia using high-resolution satellite imagery. Ecohydrology 12, 1–18. https://doi.org/10.1002/eco.2126

Deb, J.C., Phinn, S., Butt, N., McAlpine, C.A., 2018.

Climate change impacts on tropical forests: Identifying risks for tropical Asia. J. Trop. For. Sci. 30, 182–194. https://doi.org/10.26525/jtfs2018.30.2.182194

Fast, J.D., Berg, L.K., Feng, Z., Mei, F., Newsom, R., Sakaguchi, K., Xiao, H., 2019. The Impact of Variable Land-Atmosphere Coupling on Convective Cloud Populations Observed During the 2016 HI-SCALE Field Campaign. J. Adv. Model. Earth Syst. 11, 2629–2654. https://doi.org/10.1029/2019MS001727

Fusami, A.A., Nweze, O.C., Hassan, R., 2020. Comparing the Effect of Deforestation Result by NDVI and SAVI. Int. J. Sci. Res. Publ. 10, 918–925. https://doi.org/10.29322/ijsrp.10.06.2020.p102110

Jensen, J.R., Lulla, K., 1987. Introductory digital image processing: A remote sensing perspective. Geocarto Int. 2, 65. https://doi.org/10.1080/10106048709354084

June, T., Meijide, A., Stiegler, C., Kusuma, A.P., Knohl, A., 2018a. The influence of surface roughness and turbulence on heat fluxes from an oil palm plantation in Jambi, Indonesia. IOP Conf. Ser. Earth Environ. Sci. 149. https://doi.org/10.1088/1755-1315/149/1/012048

June, T., Srimani Puspa Dewi, N.W., Meijide, A., 2018b. Comparison of Aerodynamic, Bowen-Ratio, and Penman-Monteith Methods in Estimating Evapotranspiration of Oil Palm Plantation. Agromet 32, 11. https://doi.org/10.29244/j.agromet.32.1.11-20

Leite-Filho, A.T., Soares-Filho, B.S., Davis, J.L., Abrahão, G.M., Börner, J., 2021. Deforestation reduces rainfall and agricultural revenues in the Brazilian Amazon. Nat. Commun. 12, 1–7. https://doi.org/10.1038/s41467-021-22840-7

Lenderink, G., Buishand, A., Van Deursen, W., 2007. Estimates of future discharges of the river Rhine using two scenario methodologies: Direct versus delta approach. Hydrol. Earth Syst. Sci. 11, 1145–1159. https://doi.org/10.5194/hess-11-1145-2007

Li, J., Mamtimin, A., Li, Z., Jiang, C., Wang, M., 2019. Effects of Summer Rainfall on the Soil Thermal Properties and Surface Energy Balances in the Badain Jaran Desert. Adv. Meteorol. 2019. https://doi.org/10.1155/2019/4960624

Liang, S., Shuey, C.J., Russ, A.L., Fang, H., Chen, M., Walthall, C.L., Daughtry, C.S.T., Hunt, R., 2003. Narrowband to broadband conversions of land surface albedo: II. Validation. Remote Sens. Environ. 84, 25–41. https://doi.org/10.1016/S0034-4257(02)00068-8

Miettinen, J., Shi, C., Liew, S.C., 2011. Deforestation rates in insular Southeast Asia between 2000 and 2010. Glob. Chang. Biol. 17, 2261–2270. https://doi.org/10.1111/j.1365-2486.2011.02398.x

Oliveira, B.S., Moraes, E.C., Carrasco-Benavides, M., Bertani, G., Mataveli, G.A.V., 2018. Improved albedo estimates implemented in the METRIC model for modeling energy balance fluxes and evapotranspiration over agricultural and natural areas in the Brazilian Cerrado. Remote Sens. 10. https://doi.org/10.3390/rs10081181

Othman, M.A., Ash'Aari, Z.H., Aris, A.Z., Ramli, M.F., 2018. Tropical deforestation monitoring using NDVI from MODIS satellite: A case study in Pahang, Malaysia. IOP Conf. Ser. Earth Environ. Sci. 169, 1–10. https://doi.org/10.1088/1755-1315/169/1/012047

Rustiadi, E., Barus, B., Iman, L.S., Mulya, S.P., Pravitasari, A.E., Antony, D., 2018. Land use and spatial policy conflicts in a rich-biodiversity rain forest region: The case of Jambi Province, Indonesia. Springer Geogr. 277–296. https://doi.org/10.1007/978-981-10-5927-8_15

Sabajo, C.R., Le Maire, G., June, T., Meijide, A., Roupsard, O., Knohl, A., 2017. Expansion of oil palm and other cash crops causes an increase of the land surface temperature in the Jambi province in Indonesia. Biogeosciences 14, 4619–4635. https://doi.org/10.5194/bg-14-4619-2017

Scott, C.E., Monks, S.A., Spracklen, D. V., Arnold, S.R., Forster, P.M., Rap, A., Äijälä, M., Artaxo, P., Carslaw, K.S., Chipperfield, M.P., Ehn, M., Gilardoni, S., Heikkinen, L., Kulmala, M., Petäjä, T., Reddington, C.L.S., Rizzo, L. V., Swietlicki, E., Vignati, E., Wilson, C., 2018. Impact on short-lived climate forcers increases projected warming due to deforestation. Nat. Commun. 9, 1–9. https://doi.org/10.1038/s41467-017-02412-4

Takahashi, A., Kumagai, T., Kanamori, H., Fujinami, H., Hiyama, T., Hara, M., 2017. Impact of tropical deforestation and forest degradation on precipitation over Borneo Island. J. Hydrometeorol. 18, 2907–2922. https://doi.org/10.1175/JHM-D-17-0008.1

Winckler, J., Reick, C.H., Bright, R.M., Pongratz, J., 2019. Importance of Surface Roughness for the Local Biogeophysical Effects of Deforestation. J. Geophys. Res. Atmos. 124, 8605–8618. https://doi.org/10.1029/2018JD030127

Yanuar, R.C., Hanintyo, R., Muzaki, A.A., 2018. Penentuan Jenis Citra Satelit Dalam Interpretasi Luasan Ekosistem Lamun Menggunakan Pengolahan Algoritma Cahaya Tampak. J. Ilm. Geomatika 23,

75. https://doi.org/10.24895/jig. 2017.23-2.704

Zaitunah, A., Samsuri, S., Ahmad, A.G., Safitri, R.A., 2018. Normalized difference vegetation index (ndvi) analysis for land cover types using landsat 8 OLI in besitang watershed, Indonesia. IOP Conf. Ser. Earth Environ. Sci. 126. https://doi.org/10.1088/1755-1315/126/1/012112

Zeng, J., Zhang, Q., 2020. The trends in land surface heat fluxes over global monsoon domains and their responses to monsoon and precipitation. Sci. Rep. 10, 1–15. https://doi.org/10.1038/s41598-020-62467-0